Received: 16 January 2024 | Revised: 18 July 2024 | Accepted: 21 July 2024

DOI: 10.1002/app.56091

RESEARCH ARTICLE

Applied Polymer SCIENCE WILEY

# Environmental aging influence on mechanical properties of additive manufactured polyamide parts: A statistical approach

**Chahine Ghimouz** | **Jean Pierre Kenné** | **Lucas A. Hof**

Mechanical Engineering Department, École de technologie supérieure, Montreal, Québec, Canada

**Correspondence**
Lucas A. Hof, Mechanical Engineering Department, École de technologie supérieure, 1100, rue Notre-Dame Ouest, Montreal, Québec H3C1K3, Canada.
Email: lucas.hof@etsmtl.ca

**Funding information**
Natural Sciences and Engineering Research Council of Canada, Grant/Award Numbers: RGPIN-2018-05292, RGPIN-2019-05973; Mitacs, Grant/Award Number: IT28262

**Abstract**

This study explores the influence of environmental factors and printing orientation on the aging of additive manufactured polyamide 12 (PA12). A multifactorial experimental design was employed to age specimens under controlled conditions. Analysis of variance revealed that temperature, irradiance, relative humidity, and time significantly impact the ultimate tensile strength (UTS) and Young's modulus ($Y$) of PA12. Applying multiple linear regression methods produced predictive models with $R^2$ values of 0.9075 for the UTS and 0.5226 for the $Y$, indicating substantial explanatory power for the specimen's UTS. These models enhance understanding of PA12 aging, aiding in the design of more durable mechanical parts for applications exposed to environmental conditions, such as footwear, automotive components, and medical devices. As next steps, future research could empirically deploy these developed predictive models and explore longer time scales to further elucidate the long-term aging behavior of additively manufactured PA12.

**KEYWORDS**

aging, degradation, manufacturing, mechanical properties, polyamides

## 1 | INTRODUCTION

Polymers, a divers class of materials, can be categorized into thermoplastics, thermosets, and elastomers. Although thermoplastic polymers are commonly known as plastics, thermosets are often referred to as resins, and elastomers are known as rubbers. These materials have undergone extensive development and study since the early twentieth century and have been mass-produced for nearly a century.[1] Their low mass, high flexibility, and ease of shaping resulted in a wide range of applications of polymer materials in engineering fields.

Compared to the long history of polymer engineering processes, additive manufacturing (AM), introduced in the 1980s, is still an emerging manufacturing process that has not yet reached its maturity.[2,3] Among the seven (7) primary AM technologies outlined in the ISO/ASTM 52900:15 standard,[4] polyamide 12 (PA12 or Nylon 12) powder bed fusion (PBF) stands out as the most developed category for industrial product applications.[5,6] The most widely deployed polymer AM technologies for PBF in industry are Multi Jet Fusion (MJF),[7,8] and selective laser sintering (SLS).[7,8] SLS employs a laser for melting and fusing the feedstock powder, contrary to the MJF process that fuses the powder to produce final parts by

using infrared light, heat and a bonding agent. Both methods involve heating particles of feedstock powder, typically ranging in size from 45 to 90 μm,[9] in order to sinter and consolidate these particles layer by layer, ultimately forming a three-dimensional (3D) object.

In contrast to traditional manufacturing methods, AM offers a significant level of geometric freedom in both design and fabrication.[10] PBF AM processes present various advantages, including mass customization, lightweight, surface texturing, and precise dimensional accuracy.

Polymer AM has found application in diverse fields, such as the medical industry,[11] the aerospace sector, and the automotive industry,[10] as well as spare parts for maintenance and repair,[12] or as a process that can be integrated into the design and manufacture of footwear with the aim of reducing its environmental impact.[13] Among the limitations associated with the PBF process is the generation of residual stresses in the produced part, due to temperature graduations created by the layer-by-layer sintering, which can result in warping, as well as dimensional and shape deviations of the final part. Furthermore, although reducing the manufacturing process speed, post-processing is often necessary in most industrial scenarios to achieve a satisfactory surface finish, for example, to increase the fatigue resistance of printed parts.

The composition of feedstock polymer powders used in AM can vary significantly depending on the manufacturer, resulting in particles with different morphologies such as spherical, flaky, rounded, or irregular shapes.[15] Moreover, these particles also exhibit heterogeneous sizes, leading to variations in packing density and, consequently, the final density of the additively manufactured parts. This variation in density directly influences the mechanical properties of the fabricated component.

In addition, it is essential to consider the material's degradation as a significant process factor, especially when reusing powder over multiple cycles.[12] Indeed, one notable vulnerability of polymers is their susceptibility to degradation caused by environmental factors, commonly known as weathering.[13]

Polymers are formed through the polymerization process, wherein short monomers are chemically bonded to create long molecular chains comprising tens of thousands of monomers. However, prolonged exposure to environmental factors, including heat, humidity, and ultraviolet (UV) radiation, can induce structural degradation within these polymer chains. The degradation mechanisms encompass various types such as thermal, ozone-induced, photo-oxidative, mechanochemical, biodegradation, and catalytic degradation among others.[14] It is essential to note that all these degradation mechanisms can adversely affect the mechanical properties of the polymer, which is discussed in detail in literature.[15] Hence, the influence of weathering on polymers has been a subject of investigation since the 1950s.[13]

In order to simulate the environmental stresses that polymers experience, specialized equipment for accelerated weathering has been developed, enabling laboratories to replicate and study the effects of these stresses on polymers. The literature offers abundant studies on the aging of injection molded polymers, however, aging studies for PBF fabricated parts are limited. In fact, aging studies were most often carried out during the manufacturing process to understand the degradation of the powder and the impact of mixing recycled with virgin powder on the mechanical properties of the final part.

Various studies in the literature have added to the understanding of material aging in PBF-manufactured components. For instance, research has explored the degradation of SLS fabricated PA12 parts after accelerated Ultraviolet B (UVB) exposure,[16] investigated the impact of water conditioning on the fracture behavior of composite PA12 parts,[17] and compared the effects of heat conditioning on SLS and injection molded parts.[18] A recent comprehensive study evaluated the effect of accelerated weathering of different materials on their mechanical properties based on method A of the ISO-4982-3 standard,[19] which involves an Ultraviolet A (UVA)-340 radiation at 0.76 W $m^{-2}$ under an exposure at a temperature of 60°C during 8 h, followed by a 4 h condensation phase at 50°C and repeating these 12 h cycles for a total duration of 1500 h.[20] However, the protocol provided by this standard does not allow the evaluation of the direct effect of each factor independently of the others (e.g., temperature, relative humidity, and ultraviolet light irradiance) nor their combined effect on polymer degradation, because of the different environmental factors.

In the context of sustainable manufacturing, improved understanding of the effect of aging on additively manufactured (polymer) materials is needed to design parts that consider their mechanical properties over time, that is, their durability. A major current knowledge gap in this research field is the study of the individual and combined effect of environmental factors on polymer AM part performance. Therefore, this study aims to address this research gap by establishing an experimental design to assess the independent effect of each environmental factor contributing to material degradation, as well as to evaluate the combined binary effect of the different independent environmental variables.

In addition, the performed assessment includes an evaluation of vapor polishing as a post-processing technique for PA12 AM parts. This evaluation compares the mechanical properties and weathering resistance between samples that underwent vapor polishing and those that remained as-built.

## 2 | MATERIALS AND METHODS

The developed methodology for this study consists of four (4) stages that are presented in Figure 1 and discussed in the Sections 2.1–2.4. In a first step (Section 2.1), the specimens for material degradation tests are prepared, whereas a second step (Section 2.2) involves the development of the experimental design for the weathering tests, detailing both the dependent and independent variables. The third stage (Section 2.3) includes the tensile tests to determine the mechanical properties after each weathering test. Finally, in step four (Section 2.4), the results are thoroughly analyzed by statistical methods to reveal interactions between the different experimental factors.

### 2.1 | Sample preparation

Tensile tests were required to estimate the mechanical properties, ultimate tensile strength (UTS) and Young's modulus ($Y$), in this work. Therefore, tensile test specimens were designed according to the ASTM D638 Type 1 standard, as presented in Figure 2a.[21] All specimens were printed from virgin polyamide 12, also referred to as PA12 or PA 2200, powder from EOS GmbH on an EOS P110 SLS printer with a chamber temperature of 168°C.

The selected polyamide material is a semi-crystalline polymer, exhibiting material properties, such as outlined in Table 1.

Figure 2b presents a screenshot of the build chamber preparation; the XYZ and XZY oriented specimens are uniformly distributed over the entire height of the chamber to reduce the effect of hypothetical temperature variations of the parts. Before further treatment, the specimens were shuffled and picked in random order to have a better statistical representation for next steps. A vapor polishing (Vp) treatment, performed by the supplier AMTechnologies (AMT),[27] was applied to half of the total number of specimens (135) in order to experimentally estimate its protective effect on the aging of their surface condition. Table 2 summarizes the characteristics of the PBF fabricated and Vp treated PA 2200 specimens for this study.

### 2.2 | Accelerated weathering

An experimental design was developed including six (6) two-level factors applied on a total of 276 samples. The factors selected in this study for accelerated aging are chamber temperature (temperature), relative humidity, irradiance at 340 nm, exposure time (time), and vapor polishing and layer orientation during printing. The dependent variables for this study are UTS and Young's modulus ($Y$).

A two-level fractional factorial experimental design was selected in order to avoid over costly and lengthy experiments and its details are presented in Table 3 and Figure 3. The weathering was performed on a Q-Sun Xe-3 Xenon Test Chamber using UVA lamps with a wavelength of 340 nm.[28] A single cycle was performed on the specimens in each configuration, and the machine was recalibrated every 500 h. The specimens were flipped to the other side in the middle of each cycle to have a homogeneous aging on both sides of each sample.

Due to the seasonality of solar irradiance, the choice of irradiance levels was based on average measured values according to the summer (June) and winter season (December). Details of such measurements are presented in more detail in literature.[29]

Regarding the temperature, the two levels of 30 and 70°C for the experimental design, were chosen based on

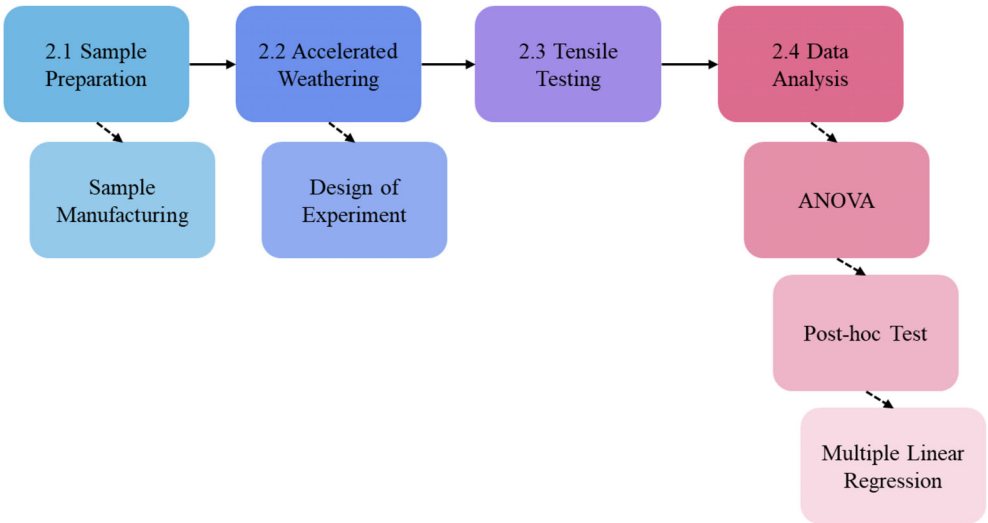


**FIGURE 1** Schematic overview of the experimental and statistical analysis methodology adopted in this study. [Color figure can be viewed at wileyonlinelibrary.com]

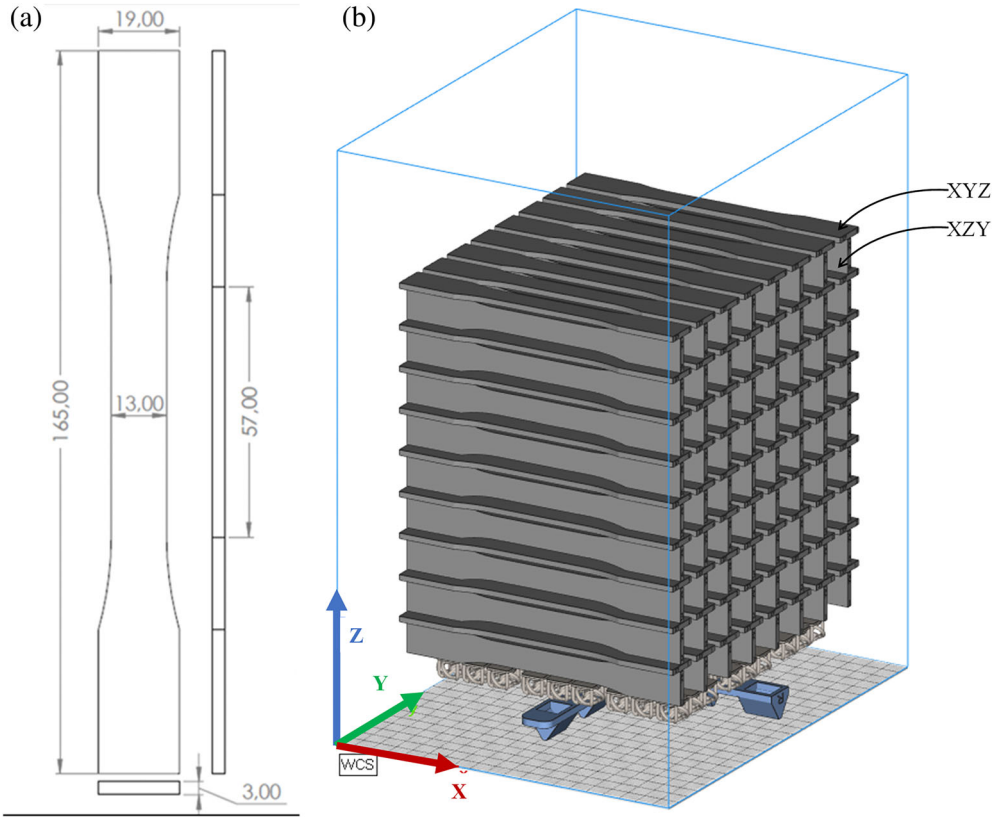


**FIGURE 2** (a) ASTM D638-Type 1 specimen dimensions (mm), (b) build orientation XYZ and XZY. [Color figure can be viewed at wileyonlinelibrary.com]

**TABLE 1** Key material properties of PA 2200.

| Properties | Values |
|---|---|
| Chemical formula[22] | $[(CH_2)_{11}CONH]_n$ |
| Density[23] | 0.93 g $cm^{-3}$ |
| Melting temperature ($T_m$)[23,24] | 176–178°C |
| Glass transition temperature ($T_g$)[22,24,25] | 42–54°C |
| Degree of crystallinity ($D_c$)[22] | 57% |
| Average molecular weight ($M_{\overline{w}}$)[25,26] | 18,900–32,900 g $mol^{-1}$ |

the glass transition temperature of PA2200 as presented in Table 1.

Concerning the relative humidity, and time, two levels were chosen that allowed for a measurable effect of each factor and that exceeded the variability of mechanical properties due to the SLS manufacturing process.[30] The choice of the used, typical, values for the levels is based on complementary studies found in the literature.[31,32]

Figure 3 shows the fractional multifactorial experimental design that was developed, including the total number of specimens (276) of which 32 specimens (11.6%) served as reference, that is, without aging treatment. Regarding the aging treatment, eight (8) different configurations were tested (C1–C8), which is also illustrated in Figure 3. Table 3 presents the different levels of each independent variable for the eight (8) configurations with the corresponding number ($n$) of aged specimens specified in Figure 3.

## 2.3 | Tensile testing

The tensile tests performed on the samples were carried out in accordance with the ASTM D638-22 Type 1 standard,[21] employing a 10kN load cell on an MTS Alliance RF/200 machine at a temperature of 23°C and 50% humidity. The displacement speed was set to 5 mm/min and the displacement data acquisition frequency was 10 Hz with the same operator performing all the tests presented in this study. The exact dimensions (width and thickness) of the specimens were entered into the MTS software for each tested specimen to avoid dimensional variations by the manufacturing process and by the applied weathering treatments. The specimens were directly placed in vacuum sealed bags and stored at 20°C in a dark storage place after being removed from the accelerated weathering machine until the tensile tests were performed, to avoid any uncontrolled aging of the specimens between the different testing operations.

**TABLE 2** Overview of the prepared specimens.

| Materials | Supplier | Process | Orientation | Machine | Dimensions | Surface | Color |
|---|---|---|---|---|---|---|---|
| PA 2200 | EOS GmbH | SLS | XYZ | EOS P110 | ASTM D638-1 | As printed | White |
| PA 2200 | EOS GmbH | SLS | XZY | EOS P110 | ASTM D638-1 | As printed | White |
| PA 2200 | EOS GmbH + AMT | SLS | XYZ | EOS P110 | ASTM D638-1 | Vapor smoothed | White |
| PA 2200 | EOS GmbH + AMT | SLS | XZY | EOS P110 | ASTM D638-1 | Vapor smoothed | White |

**TABLE 3** Levels for each factor.

| Factor | | Temperature(°C) | Relative humidity (%) | Irradiance (W $m^{-2}$ $nm^{-1}$) | Time h | Vapor polishing | Build orientation |
|---|---|---|---|---|---|---|---|
| Levels | 1 | 30 | 50 | 0.23 | 250 | No | XYZ |
| | 2 | 70 | 80 | 0.68 | 500 | Yes | XZY |

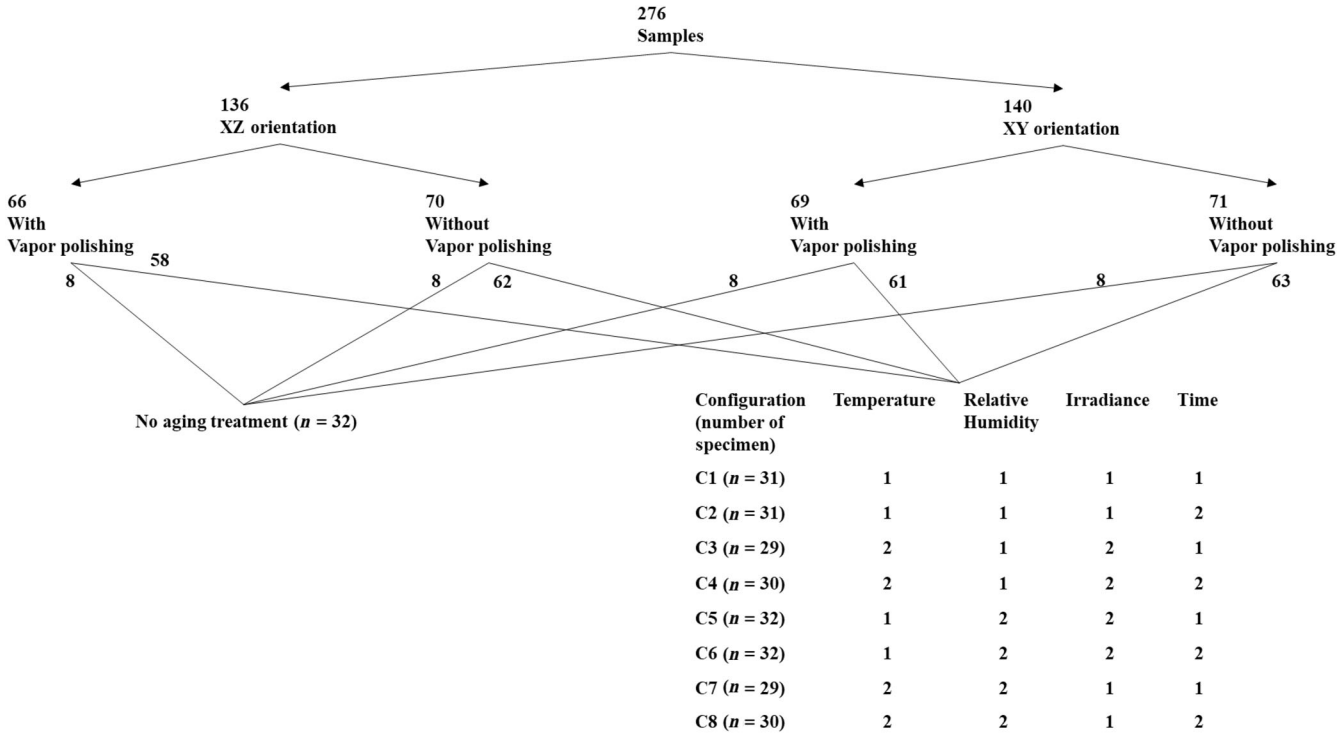


**FIGURE 3** Presentation of the fractional multifactorial experimental design.

## 2.4 | Data analysis

For each factor level configuration (C1–C8), the number of specimens tested ($n$) is presented in the first column of Table A.1 in in Data S1 with a total of 244 specimens tested in addition to the 32 reference specimens.

Table 6 summarizes the UTS and $Y$ results for the two levels of each factor, including absolute frequencies. The collected data of the tensile results (UTS and Y) were then analyzed by analysis of variance (ANOVA) to determine the significance of the individual and combined effects of the independent variables (temperature, irradiance, relative humidity, time, presence of surface treatment by vapor polishing and build orientation) with a 95% confidence level. To further analyze the interactions, a post-hoc pairwise comparison (Tukey test[33]) was carried out for each interaction. This included examining the effects of the combined binary factors as detailed in Table 3.

A multiple linear regression (MLR) model for the prediction of UTS and $Y$ is proposed, composed of the independent variables and their possible interactions, based on the ANOVA results. When multiple models needed to be compared, the Akaike criterion (AIC),[34] was used to estimate the relative quality of each proposed model. It should be noted that the health of the presented models

will be diagnosed by checking the assumptions of linearity, absence of autocorrelation, homoscedasticity, normality of the error term, absence of multicollinear values, as well as the absence of influential values using the Cook distance.[35,36] The coefficients of each independent and interaction variable will be presented and interpreted along with their associated *p*-values.

The variance of the dependent variables (UTS and Y) by the independent variables (temperature, irradiance, relative humidity, time, vapor polishing and build direction) was evaluated for the proposed MLR models using the coefficient of determination $R^2$ and adjusted $R^2$ metrics. $R^2$ adjustment is used to penalize the number of predictors used in MLR models, and the $R^2$ and adjusted $R^2$ values were calculated by Equation 1 and 2, where $n$ is the number of observations, and $k$ is the number of predictors

$$R^2 = 1 - \frac{SS_{res}}{SS_{total}}, \quad (1)$$

$$R^2{}_{Adjusted} = 1 - (n-1)\frac{\left(\frac{SS_{res}}{SS_{total}}\right)}{(n-k)}, \quad (2)$$

where $SS_{res}$ is the sum of squared residuals, and $SS_{total}$ is the total sum of the squares, as denoted in Equation 3 and 4, respectively.

$$SS_{res} = \sum_{1}^{n} (y - y^*)^2, \quad (3)$$

$$SS_{total} = \sum_{1}^{n} (y - \bar{y})^2, \quad (4)$$

where $y$ is the individual observed value, $y^*$ is the individual predicted value, and $\bar{y}$ is the overall mean.

## 3 | RESULTS AND DISCUSSION

Reference tests were carried out on eight (8) specimens per category that had not received any aging treatment, as summarized in Table 4. As discussed in the introduction, AM implies a greater or lesser variability of mechanical properties depending on the control of manufacturing parameters,[37,38] and the properties of the deployed powder[39]

It can be observed from Table 4, that the coefficient of variation (CoV) is relatively low for the UTS, which indicates a good repeatability as well as for the *Y* that has a CoV between 6.67% and 9.56%, which corresponds to the coefficient determined by Faes et al. between 5.61% and 6.5%.[30]

After the ANOVA of the reference results presented in Table 4, Table 5 demonstrates that the surface

**TABLE 4** Mechanical properties of PA2200 printed specimens without aging treatment in orientations flat (XYZ) and on edge (XZY) with and without Vp.

| | | XYZ as printed | XYZ Vp | XZY as printed | XZY Vp |
|---|---|---|---|---|---|
| UTS MPa | Mean (SD) | 52.01 (0.41) | 54.10 (0.70) | 48.95 (0.62) | 51.73 (0.39) |
| | CoV | 0.79 | 1.31 | 1.27 | 0.77 |
| | Min/max | 51.30/52.40 | 52.80/55.00 | 48.10/50.10 | 51.20/52.30 |
| Y MPa | Mean (SD) | 2135.82 (142.64) | 2093.04 (48.93) | 2179.88 (208.59) | 2011.02 (154.95) |
| | CoV | 6.67 | 2.33 | 9.56 | 7.70 |
| | Min/max | 1933.42/2323.84 | 2031.78/2164.71 | 1811.45/2467.05 | 1856.23/2283.04 |
| Elongation at break % | Mean (SD) | 18.82 (2.59) | 18.90 (2.03) | 21.68 (3.42) | 20.91 (2.14) |
| | CoV | 13.79 | 10.76 | 15.80 | 10.25 |
| | Min/max | 15.30/23.20 | 16.10/21.90 | 15.90/26.90 | 18.50/23.90 |

**TABLE 5** ANOVA for mechanical properties of PA2200 printed samples without aging treatment in orientations flat (XYZ) and on edge (XZY) with and without Vp.

| UTS | | Young's modulus | | Elongation at break | |
|---|---|---|---|---|---|
| **Factors** | ***p*-value** | **Factors** | ***p*-value** | **Factors** | ***p*-value** |
| A: Vapor polishing | <0.0001 | A: Vapor polishing | 0.0562 | A: Vapor polishing | 0.7072 |
| B: Build direction | <0.0001 | B: Build direction | 0.7235 | B: Build direction | 0.0133 |
| Interactions | | Interactions | | Interactions | |
| AB | 0.0843 | AB | 0.2452 | AB | 0.6486 |

treatment by Vp significantly increases the mechanical strength (UTS) for any printing orientation with a $p$-value <0.0001. Regarding the elongation, only the orientation of the part during printing influences this property with a $p$-value = 0.0133. The Young's modulus ($Y$) is not significantly affected by either Vp nor part orientation during printing. No interaction between Vp and part orientation is observed for the three dependent variables.

Table 6 presents a description of the data provided by the tensile tests on aged samples for both levels of the different factors by presenting the mean (Mean), standard deviation (SD), minimum (Min), maximum (Max), and absolute frequencies ($n$). It should be noted that the averages in Table 6 are not representative for the individual effect of each factor; in fact, here the effect of other factors is not considered to describe the dependent variables UTS and $Y$. However, the evolution of the average values is in good agreement with the literature.[20]

Figure 4 shows the variation of the $Y$ according to the eight configurations (C1–C8) presented in Section 2.2 for the four (4) studied cases, including Vp and as-built samples, as well as different printing orientations. It can be noticed that for all the configurations, the Vp treatment increases the stiffness for PA12 for the XYZ and XZY construction orientation. It can also be observed that for PA12 with Vp treatment and as printed in the XYZ orientation typically results in a higher median of $Y$ compared to the XZY orientation printed samples. Indeed, due to variability depending on the treatment conditions the median of $Y$ varies significantly. The ANOVA described in Section 3.1 suggests that it is required to evaluate the direct influence of the independent variables as well as their interactions, thus it is not necessary to look at the levels of the dependant variable $Y$.

The variation of the UTS values according to the different aging treatment configurations is presented in Figure 5, which demonstrates that for some configurations (C1–C8) the effect of Vp increases the value of UTS, whereas for other configurations leaving the specimens in as printed condition resulted in a higher mechanical resistance. This is caused by the interaction effect of the independent variables (temperature, relative humidity, irradiance, vapor polishing, build orientation, and time), which justifies further investigation by the ANOVA method. Furthermore, it was noticed that the XYZ printing orientation systematically gives a higher UTS than the XZY orientation and this for any configuration, with or without Vp.

## 3.1 | Analysis of variance

In view of the limited number of performed configurations, three different models (Model 1, Model 2, and Model 3) are analyzed to determine the effect of the factors on the dependent variables UTS and Y. These models include five (5) factors each, indeed, the time, Vp treatment, and different build orientations (XYZ and XZY) are treated in each model. Tables 7.a and 8.a present the ANOVA results indicating the significance of the effect of the independent factors as well as the significant interactions whose $p$-values are lower than 0.05 (highlighted in red).

For the three developed models, the $p$-values of the ANOVA indicate a significant effect of the factors used in the models on the mechanical strength of the tested

**TABLE 6** Data description for aged samples: ultimate tensile strength (UTS) and Young's modulus ($Y$) for each factor level.

| | | UTS (MPa) | | | Y (MPa) | | |
|---|---|---|---|---|---|---|---|
| | **Levels** | **Min** | **Max** | **Mean (SD)** | **Min** | **Max** | **Mean (SD)** |
| Temperature (°C) | 30 ($n$ = 126) | 35.80 | 53.60 | 48.77 (2.97) | 1745.80 | 2604.53 | 2073.92 (172.87) |
| | 70 ($n$ = 118) | 10.80 | 47.90 | 31.82 (9.21) | 1640.25 | 4846.26 | 2262.75 (428.08) |
| Relative humidity (%) | 50 ($n$ = 137) | 10.80 | 53.60 | 39.35 (12.16) | 1745.80 | 4846.26 | 2269.29 (373.71) |
| | 80 ($n$ = 107) | 22.70 | 50.80 | 42.14 (8.65) | 1640.25 | 2674.55 | 2032.02 (216.60) |
| Irradiance (W $m^{-2}$ $nm^{-1}$) | 0.23 ($n$ = 121) | 22.70 | 53.60 | 44.26 (9.13) | 1640.25 | 2674.55 | 2037.32 (217.60) |
| | 0.68 ($n$ = 123) | 10.80 | 50.80 | 36.95 (11.18) | 1828.54 | 4846.26 | 2291.10 (381.31) |
| Time (h) | 250 ($n$ = 121) | 22.70 | 53.40 | 41.27 (10.50) | 1640.25 | 3315.56 | 2149.18 (278.04) |
| | 500 ($n$ = 123) | 10.80 | 53.60 | 39.89 (11.16) | 1723.05 | 4846.26 | 2181.04 (384.22) |
| Vapor polishing No/Yes | No ($n$ = 125) | 18.00 | 51.70 | 41.93 (10.19) | 1640.25 | 3193.13 | 2076.70 (284.81) |
| | Yes ($n$ = 119) | 10.80 | 53.60 | 39.15 (11.34) | 1805.03 | 4846.26 | 2258.24 (359.86) |
| Build orientation XYZ/XZY | XYZ ($n$ = 124) | 18.00 | 53.60 | 41.18 (11.14) | 1693.96 | 3315.56 | 2185.26 (308.48) |
| | XZY ($n$ = 120) | 10.80 | 52.10 | 39.95 (10.51) | 1640.25 | 4846.26 | 2144.56 (361.40) |

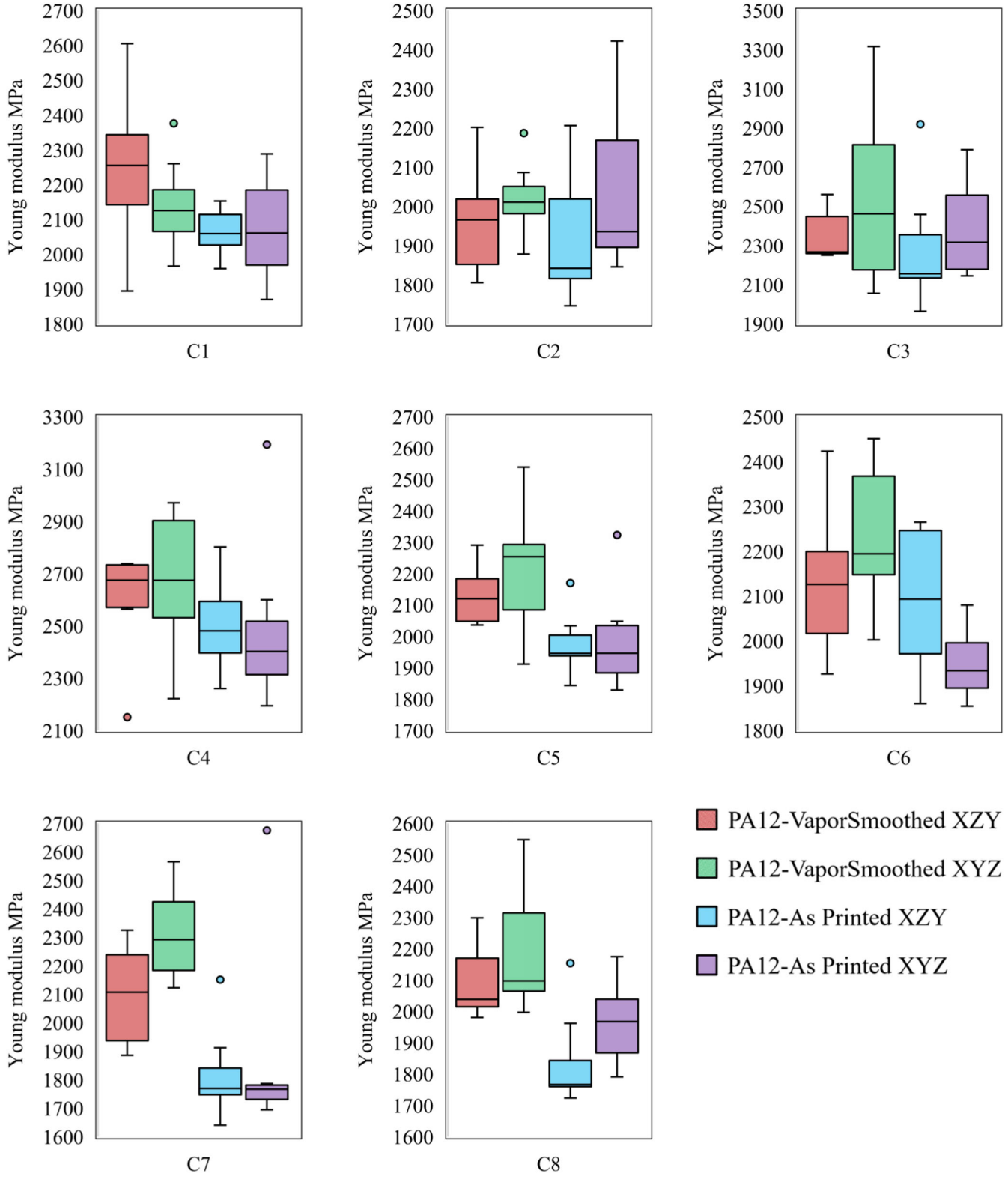


**FIGURE 4** Variation of Young's modulus ($Y$) as a function of aging conditions C1–C8 (see for definitions Figure 3) for samples with/without vapor polishing and according to the building orientation. [Color figure can be viewed at wileyonlinelibrary.com]

specimens (Table 7.a). Regarding the Young's modulus (Table 8.a), it is noticed that in the three models the two (2) factors (time and part orientation during printing) do not have a direct significant effect on $Y$ ($p$-value >0.05).

In Table 7.a it can be clearly concluded that beyond the individual effects of the factors, there is also the effect of the binary interactions between the different factors which is statistically significant. In the purpose of

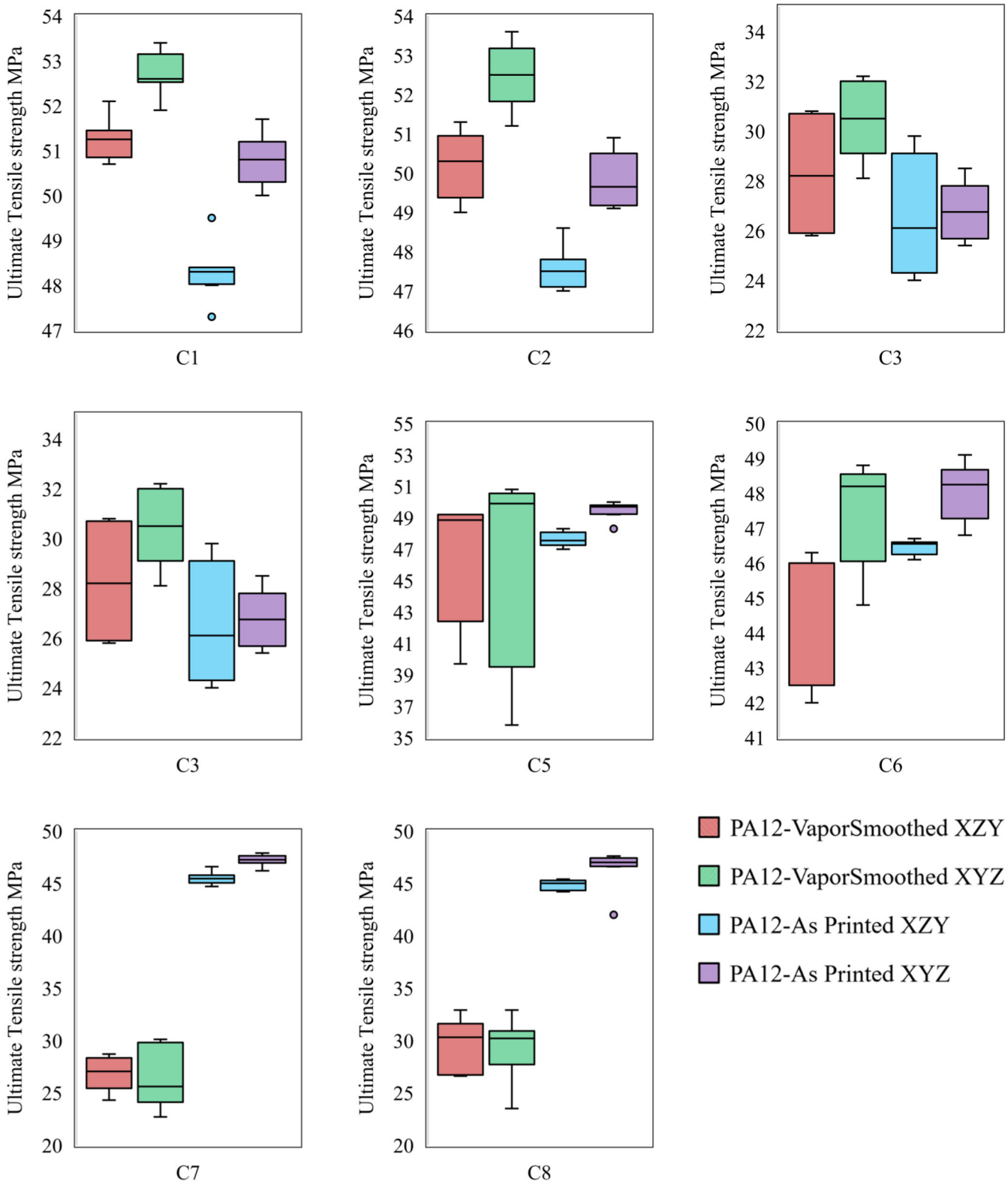


**FIGURE 5** Variation of ultimate tensile strength (UTS) as a function of aging conditions C1–C8 (see for definition in Figure 3) for samples with/without Vapor polishing and according to the building orientation. [Color figure can be viewed at wileyonlinelibrary.com]

studying and understanding the interactions multiple pairwise comparisons (post hoc tests) are proposed.

Table 7.b demonstrates that the interaction effect of the pair of factors (temperature/relative humidity) affect the UTS significantly in both directions, that is, when the temperature is set at any level the effect of relative humidity differs, which is supported by a *p*-value less than 5%. In the case where we fix the relative humidity at

**TABLE 7.a** Results of the ANOVA of the three models for UTS.

| | UTS | | | | | | | |
|---|---|---|---|---|---|---|---|---|
| | **Factors** | ***p*-value** | | **Factors** | ***p*-value** | | **Factors** | ***p*-value** |
| Model 1 | A: Temperature | <0.0001 | Model 2 | A: Temperature | <0.0001 | Model 3 | A: Irradiance | <0.0001 |
| | B: Relative Humidity | <0.0001 | | B: Irradiance | <0.0001 | | B: Relative Humidity | 0.0010 |
| | C: Time | <0.0001 | | C: Time | 0.0172 | | C: Time | 0.8717 |
| | D: Vapor polishing | <0.0001 | | D: Vapor polishing | <0.0001 | | D: Vapor polishing | 0.0011 |
| | E: Build direction | 0.0034 | | E: Build direction | 0.0114 | | E: Build direction | 0.0122 |
| | Interactions | | | Interactions | | | Interactions | |
| | AB | <0.0001 | | AB | <0.0001 | | AB | <0.0001 |
| | AD | <0.0001 | | AD | <0.0001 | | AD | <0.0001 |
| | BD | <0.0001 | | BD | <0.0001 | | BD | <0.0001 |
| | | | | BC | 0.0103 | | | |

**TABLE 7.b** Post hoc test for interactions that affect UTS.

| **UTS (MPa)** | | | | | | | | | |
|---|---|---|---|---|---|---|---|---|---|
| Temperature (°C) | Relative humidity (%) | | | | Relative humidity (%) | Temperature(°C) | | | |
| | 50 (*i*) | 80 (*j*) | (*i*–*j*) | *p*-value | | 30 (*i*) | 70 (*j*) | (*i*–*j*) | *p*-value |
| 30 | 49.56 | 47.48 | 2.08 | 0.0001 | 50 | 49.56 | 25.86 | 23.7 | <0.0001 |
| 70 | 25.86 | 37.79 | −11.93 | <0.0001 | 80 | 47.48 | 37.79 | 9.69 | <0.0001 |
| Temperature (°C) | Vapor polishing | | | | Vapor polishing | Temperature°C | | | |
| | No (*i*) | Yes (*j*) | (*i*–*j*) | *p*-value | | 30 (*i*) | 70 (*j*) | (*i*–*j*) | *p*-value |
| 30 | 48.49 | 49.03 | −0.54 | 0.3074 | No | 48.49 | 35.47 | 13.02 | <0.0001 |
| 70 | 35.74 | 27.64 | 8.10 | <0.0001 | Yes | 49.03 | 27.64 | 21.39 | <0.0001 |
| Relative humidity (%) | Vapor polishing | | | | Vapor polishing | Relative humidity (%) | | | |
| | No (*i*) | Yes (*j*) | (*i*–*j*) | *p*-value | | 50 (*i*) | 80 (*j*) | (*i*–*j*) | *p*-value |
| 50 | 36.66 | 41.51 | −4.85 | 0.0199 | No | 36.66 | 46.95 | −10.29 | <0.0001 |
| 80 | 46.95 | 34.97 | 11.98 | <0.0001 | Yes | 41.51 | 34.97 | 6.54 | 0.0022 |
| Irradiance (W $m^{-2}$ $nm^{-1}$) | Temperature(°C) | | | | Temperature(°C) | Irradiance (W $m^{-2}$ $nm^{-1}$) | | | |
| | 30 (*i*) | 70 (*j*) | (*i*–*j*) | *p*-value | | 0.23 (*i*) | 0.68 (*j*) | (*i*–*j*) | *p*-value |
| 0.23 | 50.42 | 37.79 | 12.63 | <0.0001 | 30 | 50.42 | 47.16 | 3.26 | <0.0001 |
| 0.68 | 47.16 | 25.86 | 21.3 | <0.0001 | 70 | 37.79 | 25.86 | 11.93 | <0.0001 |
| Irradiance (W $m^{-2}$ $nm^{-1}$) | Vapor polishing | | | | Vapor polishing | Irradiance (W $m^{-2}$ $nm^{-1}$) | | | |
| | No (*i*) | Yes (*j*) | (*i*–*j*) | *p*-value | | 0.23 (*i*) | 0.68 (j) | (*i*–*j*) | *p-value* |
| 0.23 | 47.5 | 40.86 | 6.64 | <0.0001 | No | 47.5 | 36.45 | 11.05 | <0.0001 |
| 0.68 | 36.45 | 37.46 | −1.01 | 0.6171 | Yes | 40.86 | 37.46 | 3.40 | 0.1025 |
| Irradiance (W $m^{-2}$ $nm^{-1}$) | Time (h) | | | | Time (h) | Irradiance (W $m^{-2}$ $nm^{-1}$) | | | |
| | 250 (*i*) | 500 (*j*) | (*i*–*j*) | *p*-value | | 0.23 (*i*) | 0.68 (*j*) | (*i*–*j*) | *p*-value |
| 0.23 | 44.32 | 44.21 | 0.11 | 0.9490 | 250 | 44.32 | 38.27 | 6.05 | 0.0013 |
| 0.68 | 38.27 | 35.63 | 2.64 | 0.1925 | 500 | 44.21 | 35.63 | 8.58 | <0.0001 |
| Irradiance (W $m^{-2}$ $nm^{-1}$) | Relative humidity (%) | | | | Relative humidity (%) | Irradiance (W $m^{-2}$ $nm^{-1}$) | | | |
| | 50 (*i*) | 80 (*j*) | (*i*–*j*) | *p*-value | | 0.23 (*i*) | 0.68 (*j*) | (*i*–*j*) | *p*-value |
| 0.23 | 50.42 | 37.79 | 12.63 | <0.0001 | 50 | 50.42 | 30.2 | 20.22 | <0.0001 |
| 0.68 | 30.2 | 47.48 | −17.28 | <0.0001 | 80 | 37.79 | 47.48 | −9.69 | <0.0001 |

any level the effect of temperature on UTS is also significantly different.

The interaction between temperature and Vp is shown in Table 7.b. However, this interaction is only one-directional. The effect of Vp is not significant at a temperature of 30°C, but it is significant at 70°C. In the opposed direction, by applying the Vp treatment or not, the temperature has a significant effect on the mechanical strength of the studied material. This finding is valid for the first and second model presented in Table 7.a. Hence, this may suggest that Vp protects the material from thermal degradation (i.e., here defined as not affecting its UTS) at low temperatures (e.g., 30°C), however, at higher temperatures (e.g., 70°C) the protection from the Vp treatment is lost. Further research could be conducted to study more precisely the temperature limits for PA12 (PA2200) protection by the Vp process against thermal degradation. It should be noted that the present work entails a pairwise comparison and the effect of other factors is not considered, However, other factors and their interactions may help to explain the average values obtained when switching from the first temperature level to the second.

Another interaction (RH/Vp) is significantly bidirectional (note that the interaction is present in the first and third models), for any level of humidity the Vp to a different effect and vice versa. Same for the couple (irradiance/temperature) that is present in Model 2, for any level of either, the other factor will have a different effect on the UTS.

For a nonvapor polished material, irradiance has a significant effect while for samples that have received the Vp treatment well the effect of irradiance becomes nonsignificant which implies a line of thought on the protection of Nylon 12 by Vp treatment against photo degradation. A significant decrease in the average UTS with a $p$-value <0.0001 indicates that at 0.23 W $m^{-2}$ $nm^{-1}$, Vp has a significant effect contrary to a level of 0.68 W $m^{-2}$ $nm^{-1}$ where there is no effect on the mechanical strength.

For both levels of irradiance, the time has no effect, however for both levels of time the effect of irradiance is well present significantly and with a different effect depending on the time of exposure. It should be noted that this interaction is present only in Model 2, in the third proposed model the interaction between irradiance and time does not seem to be significant with a $p$-value equal to 0.8868.

For the interaction of the pair (irradiance/relative humidity) found in Model 3, there seems to be an effect of both factors for any level of the other. Hence, a bidirectional interaction is observed.

Table 8.a shows the presence of significant binary interactions between the different factors for each model. As for the mechanical strength (UTS) a post-hoc test was performed on the collected data of the Young's modulus ($Y$) and shown in Table 8.b.

As can be observed in Table 8.b the effect of the interaction between temperature and relative humidity is not significantly manifested for all configurations, for a temperature of 70°C, the increase in the level of relative humidity lowers the Young's modulus of Nylon 12. However, for a relative humidity of 50% the increase in temperature makes the material stiffen increasing the Young's modulus in this model.

Regarding the interaction of temperature and Vp treatment, the results show that Vp treatment protects the material from thermal degradation for both tested temperature levels. Time seems to have an effect only for long exposure times, in such cases, we observe a difference of $Y$ between the two temperature levels.

**TABLE 8.a** Results of the ANOVA of the three models for Young's modulus.

| | Y | | | | | | | |
|---|---|---|---|---|---|---|---|---|
| | **Factors** | ***p*-value** | | **Factors** | ***p*-value** | | **Factors** | ***p*-value** |
| Model 1 | A: Temperature | <0.0001 | Model 2 | A: Temperature | <0.0001 | Model 3 | A: Irradiance | <0.0001 |
| | B: Relative Humidity | <0.0001 | | B: Irradiance | <0.0001 | | B: Relative Humidity | <0.0001 |
| | C: Time | 0.3419 | | C: Time | 0.3102 | | C: Time | 0.9475 |
| | D: Vapor polishing | <0.0001 | | D: Vapor polishing | <0.0001 | | D: Vapor polishing | <0.0001 |
| | E: Build direction | 0.1978 | | E: Build direction | 0.1906 | | E: Build direction | 0.3222 |
| | Interactions | | | Interactions | | | Interactions | |
| | AB | <0.0001 | | AB | <0.0001 | | AB | 0.0001 |
| | AC | 0.0047 | | AC | 0.0035 | | AC | 0.0330 |
| | AD | 0.0391 | | AD | 0.0342 | | BD | 0.0022 |
| | | | | BC | 0.0012 | | | |

**TABLE 8.b** Post hoc test for interactions that affect the Young's modulus (*Y*).

| **Y (MPa)** | | | | | | | | | |
|---|---|---|---|---|---|---|---|---|---|
| Temperature (°C) | Relative humidity (%) | | | | Relative humidity (%) | Temperature (°C) | | | |
| | 50 (*i*) | 80 (*j*) | (*i*−*j*) | *p*-value | | 30 (*i*) | 70 (*j*) | (*i*−*j*) | *p*-value |
| 30 | 2085.26 | 2055.50 | 29.76 | 0.3501 | 50 | 2085.26 | 2512.58 | −427.32 | <0.0001 |
| 70 | 2512.52 | 2012.93 | 499.65 | <0.0001 | 80 | 2055.5 | 2012.93 | 42.57 | 0.3143 |
| Temperature (°C) | Vapor polishing | | | | Vapor polishing | Temperature (°C) | | | |
| | No (*i*) | Yes (*j*) | (*i*−*j*) | *p*-value | | 30 (*i*) | 70 (*j*) | (*i*−*j*) | *p*-value |
| 30 | 2012.05 | 2133.85 | −121.8 | <0.0001 | No | 2012.05 | 2140.33 | −128.28 | 0.0112 |
| 70 | 2140.33 | 2402.99 | −262.66 | 0.0007 | Yes | 2133.85 | 2402.99 | −269.14 | <0.0001 |
| Temperature (°C) | Time (h) | | | | Time (h) | Temperature (°C) | | | |
| | 250 (*i*) | 500 (*j*) | (*i*−*j*) | *p*-value | | 30 (*i*) | 70 (*j*) | (*i*−*j*) | *p-value* |
| 30 | 2102.82 | 2045.02 | 57.8 | 0.0603 | 250 | 2102.82 | 2199.54 | 96.72 | 0.0556 |
| 70 | 2199.54 | 2323.86 | −124.32 | 0.1151 | 500 | 2045.02 | 2323.86 | −278.84 | <0.0001 |
| Irradiance (W $m^{-2}$ $nm^{-1}$) | Temperature (°C) | | | | Temperature (°C) | Irradiance (W $m^{-2}$ $nm^{-1}$) | | | |
| | 30 (*i*) | 70 (*j*) | (*i*−*j*) | *p*-value | | 0.23 (*i*) | 0.68 (*j*) | (*i*−*j*) | *p*-value |
| 0.23 | 2060.53 | 2012.93 | 47.6 | 0.2306 | 30 | 2060.53 | 2086.89 | −26.36 | 0.3942 |
| 0.68 | 2086.89 | 2512.58 | −425.69 | <0.0001 | 70 | 2012.93 | 2512.58 | −499.65 | <0.0001 |
| Irradiance (W $m^{-2}$ $nm^{-1}$) | Time (h) | | | | Time (h) | Irradiance (W $m^{-2}$ $nm^{-1}$) | | | |
| | 250 (*i*) | 500 (*j*) | (*i*−*j*) | *p*-value | | 0.23 (*i*) | 0.68 (*j*) | (*i*−*j*) | *p*-value |
| 0.23 | 2073.37 | 2001.85 | 71.52 | 0.0705 | 250 | 2073.37 | 2223.75 | −150.38 | 0.0026 |
| 0.68 | 2223.75 | 2357.33 | −133.58 | 0.0517 | 500 | 2001.85 | 2357.33 | −355.48 | <0.0001 |
| Irradiance (W $m^{-2}$ $nm^{-1}$) | Relative humidity (%) | | | | Relative humidity (%) | Irradiance (W $m^{-2}$ $nm^{-1}$) | | | |
| | 50 (*i*) | 80 (*j*) | (*i*−*j*) | *p*-value | | 0.23 (*i*) | 0.68 (*j*) | (*i*−*j*) | *p*-value |
| 0.23 | 2060.53 | 2012.93 | 47.6 | 0.2306 | 50 | 2060.53 | 2441.86 | −381.33 | <0.0001 |
| 0.68 | 2441.86 | 2055.5 | 386.36 | <0.0001 | 80 | 2012.93 | 2055.5 | −42.57 | 0.3143 |
| Relative humidity (%) | Vapor polishing | | | | Vapor polishing | Relative humidity (%) | | | |
| | No (*i*) | Yes (*j*) | (*i*−*j*) | *p*-value | | 50 (*i*) | 80 (*j*) | (*i*−*j*) | *p*-value |
| 50 | 2225.51 | 2304.42 | −78.91 | 0.2206 | No | 2225.51 | 1934.87 | 290.64 | <0.0001 |
| 80 | 1934.87 | 2176.62 | −241.75 | <0.0001 | Yes | 2304.42 | 2176.62 | 127.8 | 0.0625 |

It can be concluded that PA12 responds significantly to the effect of temperature for irradiance at 0.68 W $m^{-2}$ $nm^{-1}$ by increasing the average *Y* for higher temperatures. However, the irradiance has a significant effect only for a temperature of 70°C. In addition, the results show that there is an interaction between time and irradiance, the latter has a significant effect at a confidence level greater than 99% whatever the level of time used.

The interaction of irradiance with relative humidity (RH) is presented in the third model with a *p*-value less than 0.0001, the effect of RH is manifested only for an irradiance set to 0.68 W $m^{-2}$ $nm^{-1}$, as well as the effect of irradiance is manifested only for an RH of 50%.

The protective effect of the surface treatment Vp seems to be present significantly only for RH = 80%, moreover RH to a significant effect when the treatment Vp is not applied with a decrease in the mean of *Y*.

## 3.2 | Prediction model development

Based on the results of the ANOVA presented in previous sections, regression models were developed and compared with each other using the AIC in order to determine which one performs best, while penalizing the models with the largest number of independent variables. The same work was done for the explained variable UTS, as well as for *Y*. For the construction of the MLR models all the variables are numerical, except for the variable Vp and building orientation (BO). When applying the Vp treatment, the variable takes the Level 1, otherwise

0, and for the orientation on the printer build plate (XYZ) BO = 0 and for (XZY) BO = 1. As mentioned in Section 2, the models have been diagnosed and respond favorably to the assumptions of the MLR (see Appendix B in Data S1).

The proposed MLR model to predict the variation of UTS as a function of the independent variables follows the results of the ANOVA, and is expressed by Equation 5 below.

$$\mathrm{UTS} = \beta_0 + \beta_1 \mathrm{Temp} + \beta_2 \mathrm{RH} + \beta_3 \mathrm{Time} + \beta_4 \mathrm{Vp} + \beta_5 \mathrm{BO} + \beta_6 \mathrm{Temp\,RH} + \beta_7 \mathrm{Temp\,Vp} + \beta_8 \mathrm{RH\,Vp}. \quad (5)$$

Table 9 presents the coefficients ($\beta$), significance ($p$-value), standard error, and 95% confidence interval of the independent variables used in the model explaining UTS (Equation 5).

The effects of the independent variables can be estimated by considering the effect of the interactions as follows: for example, for a RH value of 50% and by increasing the temperature 1°C, the UTS will vary from $\beta_1 + \beta_6 \quad (50) = -1.1379 + (0.0125 \times 50) = -0.5145$ MPa. Thus, when a Vp treatment is applied, that is, Vp = 1, and for an increase in temperature of 1°C, the UTS will vary from $\beta_1 + \beta_7(1) = -1.1379 + (-0.1441 \times 1) = -1.282$ MPa. This reasoning can be applied to all independent variables if they interact with each other, resulting in a model with a value of the coefficient of determination $R^2 = 0.9075$ and a $R^2$ adjusted = 0.9043, which is satisfactory to validate the proposed model.

Indeed, the proposed MLR model uses the results of the ANOVA to predict the variation of $Y$ as a function of the independent variables and is expressed as follows in Equation 6:

$$\log(\mathrm{Y}) = \beta_0 + \beta_1 \mathrm{Temp} + \beta_2 \mathrm{Irr} + \beta_3 \mathrm{Time} + + \beta_4 \mathrm{Temp\,Vp} + \beta_5 \mathrm{Temp\,Irr} + \beta_6 \mathrm{Temp\,Time} + \beta_7 \mathrm{Irr\,Time}. \quad (6)$$

Table 10 presents the independent variables used in the MLR explaining $Y$, their coefficients, the standard

**TABLE 9** The values of the $p$-value, coefficients, standard errors, and 95% confidence intervals of independent variables for the model explaining ultimate tensile strength (UTS).

| | | | | | 95% confidence interval | |
|---|---|---|---|---|---|---|
| **Predicted variable** | **Independent variable** | **Coefficient** | **Std. error** | ***p*-value** | **Lower bound** | **Upper bound** |
| UTS | Constant | $\beta_0 = 81.2404$ | 3.0653 | <0.0001 | 75.2013 | 87.2796 |
| | A: Temperature | $\beta_1 = -1.1380$ | 0.0512 | <0.0001 | −1.2388 | −1.0371 |
| | B: Relative Humidity | $\beta_2 = -0.2863$ | 0.0426 | <0.0001 | −0.3702 | −0.2025 |
| | C: Time | $\beta_3 = -0.0099$ | 0.0018 | <0.0001 | −0.0134 | −0.0064 |
| | D: Vapor polishing | $\beta_4 = 29.3482$ | 2.1008 | <0.0001 | 25.2093 | 33.4871 |
| | E: Build orientation | $\beta_5 = -1.2689$ | 0.4292 | 0.0034 | −2.1145 | −0.4232 |
| | AB | $\beta_6 = 0.0125$ | 0.0007 | <0.0001 | 0.0110 | 0.0139 |
| | AD | $\beta_7 = -0.1441$ | 0.0222 | <0.0001 | −0.1878 | −0.1005 |
| | BD | $\beta_8 = -0.4139$ | 0.0301 | <0.0001 | −0.4732 | −0.3547 |

**TABLE 10** The values of the $p$-value, coefficients, standard errors, and 95% confidence intervals of independent variables for the model explaining and $Y$.

| | | | | | 95% Confidence interval | |
|---|---|---|---|---|---|---|
| **Predicted variable** | **Independent variable** | **Coefficient** | **Std. error** | ***p*-value** | **Lower bound** | **Upper bound** |
| Log ($Y$) | Constant | $\beta_0 = 7.9730$ | 0.0073 | <0.0001 | 7.8297 | 8.1170 |
| | A: Temperature | $\beta_1 = -0.0069$ | 0.0012 | <0.0001 | −0.0092 | −0.0046 |
| | B: Irradiance | $\beta_2 = -0.5886$ | 0.1104 | <0.0001 | −0.8062 | −0.3710 |
| | C: Time | $\beta_3 = -0.0007$ | 0.0002 | <0.0001 | −0.0010 | −0.0004 |
| | A×Vp | $\beta_4 = 0.0017$ | 0.0002 | <0.0001 | 0.0012 | 0.0021 |
| | AB | $\beta_5 = 0.0112$ | 0.0014 | <0.0001 | 0.0085 | 0.0139 |
| | AC | $\beta_6 = 0.0000$ | 0.0000 | 0.0018 | 0.0000 | 0.0000 |
| | BC | $\beta_7 = 0.0008$ | 0.0002 | 0.0007 | 0.0003 | 0.0012 |

error, the associated *p*-value, and the upper and lower bounds of the 95% confidence interval.

The rationale for interpretation is the same as for UTS, with one exception: the variation in $Y$ is calculated in percentage (%) rather than MPa, as the explanatory variable underwent a logarithmic transformation during model development. This was done to stabilize the variance of the variable $Y$ and reduce the effect of extreme values.

To estimate the variation of $Y$ for an irradiance fixed at $0.23\ \mathrm{W\,m^{-2}\,nm^{-1}}$, for each 1°C temperature increase, $Y$ will vary by $\beta_1+\beta_5(0.23)=100(-0.0069+(0.0112\times 0.23))=-0.4324\%$. This model has an $R^2=0.5226$ and a $R^2$ adjusted $=0.5084$.

It should be noted that these models were built to predict the UTS and $Y$ values using values of the independent variables between Level 1 and Level 2, as presented in Table 3.

The relatively low $R^2$ and adjusted $R^2$ values for the $Y$ model can be explained by the lack of factors investigated in this study. Manufacturing parameters such as the repeatability of the melt pool or the size of the powder particles have all a significant influence on the variability of the studied dependent variable $Y$, indeed, aging effects accentuate this variability.

## 3.3 | Discussion of polymer degradation mechanisms

### 3.3.1 | Temperature and relative humidity interaction

Temperature and humidity significantly impact the PA12 (PA2200) AM specimens, due to their effects on polymer chain mobility in both crystalline and amorphous phases of the polymer and intermolecular interactions.[40] Elevated temperatures increase the mobility of polymer chains, potentially lowering the glass transition temperature ($T_g$) and making the polymer more susceptible to deformation.[31,41] When combined with high humidity, the absorbed water molecules disrupt intermolecular hydrogen bonds through plasticization.[41] This reduces the polymer's tensile strength and stiffness, while increasing its flexibility and ductility. Hydrolytic degradation is also a concern at higher temperatures,[42,43] where water molecules break amide bonds, leading to a reduction in molecular weight and mechanical properties.[44]

### 3.3.2 | UV radiation and temperature interaction

The combined effects of UV radiation and high temperature accelerate the degradation of PA12 (PA2200) AM specimens. The elevated temperature may catalyze the effect of UV exposure (accelerated testing 70°C). UV exposure generates free radicals, which are more reactive at elevated temperatures. This leads to faster chain scission in the amorphous regions and oxidation,[16] hence significantly degrading mechanical properties. The synergistic interaction between UV and temperature results in more rapid loss of tensile strength, increased brittleness, and surface damage compared to each factor individually.

### 3.3.3 | UV and humidity interaction

UV radiation and high humidity together exacerbate surface degradation through photodegradation and hydrolytic processes.[16,43] Moisture absorption plasticizes the polymer and increases the rate of oxidation and chain scission under UV exposure.[16] This combination results in more severe surface cracking, discoloration, and loss of mechanical integrity.

### 3.3.4 | Additive manufactured specimens

AM introduces unique interface effects in polyamide specimens, such as layer adhesion and microstructural variations. Optical and electronic microscopy can reveal these phenomena, aiding in the understanding of mechanical and thermal behaviors. Poor interlayer adhesion can lead to reduced mechanical strength and increased susceptibility to environmental degradation.

### 3.3.5 | MLR analysis

The proposed MLR model in this study highlights the complex interactions between temperature, UV, and humidity. These interactions can be explained through established theories of polymer science (see Sections 3.3.1–3.3.4), such as the increased reactivity of free radicals at higher temperatures and the plasticizing effect of moisture. The combined effects can lead to synergistic degradation, emphasizing the importance of considering multiple environmental variables in polymer performance analysis.

The proposed prediction model is applicable to polyamide 12 (PA12) parts produced from virgin powder using SLS printing. However, for parts manufactured by other AM technologies, this model may not be valid due to inherent differences in machine-specific manufacturing parameters. Although the material degradation mechanisms remain broadly similar, the proportions of these mechanisms may vary, making the model

imprecise. Furthermore, when another material will be assessed, the MLR model, based on statistical data from samples made exclusively of PA12, loses its validity for prediction. Polymer chains, degree of crystallinity and thermal properties differ from one material to another, significantly influencing the results, as reported in tests conducted by Puttonen et al.[20]

## 4 | CONCLUSION

The experimental design developed in this work evaluated the impact of six independent variables (temperature, relative humidity, UV irradiance, time, vapor polishing, and construction orientation) on the UTS and Young's modulus ($Y$) of additive-manufactured Polyamide 12 (PA2200) specimens using SLS technology. Significant individual and interaction effects were determined through ANOVA and post hoc analysis. A MLR model, using the AIC for model selection, yielded an $R^2$ value of 0.9075 for UTS and 0.5226 for $Y$. These results inform a predictive model that enhances the optimization of fabrication processes, allowing for the adjustment of environmental parameters to achieve desired mechanical properties.

The present study fills a gap in existing knowledge and has practical implications for the AM industry. It offers a more informed approach to designing parts with enhanced longevity and durability, which is beneficial for example the automotive and medical device industries. By optimizing manufacturing parameters, manufacturers can produce parts with improved structural integrity and functional properties, minimizing the risk of premature failure and promoting sustainable manufacturing practices.

Future research should focus on experimentally testing the predictive models for UTS and $Y$, and exploring longer time scales to better understand the aging of additive manufactured materials, ultimately refining part design for long-term durability.

## AUTHOR CONTRIBUTIONS

**Chahine Ghimouz:** Conceptualization (equal); data curation (lead); formal analysis (lead); investigation (lead); methodology (lead); software (lead); validation (lead); visualization (lead); writing – original draft (lead); writing – review and editing (equal). **Jean Pierre Kenné:** Funding acquisition (supporting); resources (supporting); supervision (supporting); writing – review and editing (supporting). **Lucas A. Hof:** Conceptualization (equal); funding acquisition (lead); methodology (supporting); project administration (lead); resources (lead); supervision (lead); validation (supporting); writing – review and editing (equal).

## ACKNOWLEDGMENTS

The authors would like to acknowledge the financial support of the Natural Sciences and Engineering Research Council of Canada (NSERC) under the Discovery Grant (RGPIN-2018-05292 and RGPIN-2019-05973) as well as the financial support of the Mitacs Accelerate Grant IT28262 and ARSHAE, Montréal, Canada. Furthermore, the authors would like to thank Sylvie Gervais and Serge Vicente from the Bureau de Consultation en Statistique at École de technologie supérieure.

## CONFLICT OF INTEREST STATEMENT

The authors declare that they have no known competing financial interests or personal relationships that could have appeared to influence the work reported in this paper.

## DATA AVAILABILITY STATEMENT

The data that support the findings of this study are available in the supporting information of this article.

## ORCID

*Chahine Ghimouz* https://orcid.org/0009-0007-3781-2327
*Lucas A. Hof* https://orcid.org/0000-0002-0495-9572

## REFERENCES

[1] B. Gewert, M. M. Plassmann, M. MacLeod, *Environ Sci Process Impacts* **2015**, *17*, 1513.
[2] A. Su, S. J. Al'Aref, in *3D printing applications in cardiovascular medicine* (Eds: S. J. Al'Aref, B. Mosadegh, S. Dunham, J. K. Min), Academic Press, Boston **2018**, p. 1.
[3] H. Kodama, *Rev. Sci. Instrum.* **1981**, *52*, 1770.
[4] Additive manufacturing—General principles - Fundamentals and vocabulary (ISO/ASTM 52900:2021), ISO/ASTM, 27-04-2022. **2022**.
[5] L. J. Tan, W. Zhu, K. Zhou, *Adv. Funct. Mater.* **2020**, *30*, 2003062.
[6] F. Sillani, R. G. Kleijnen, M. Vetterli, M. Schmid, K. Wegener, *Addit. Manuf.* **2019**, *27*, 32.
[7] Y. Wu, Y. Lu, M. Zhao, S. Bosiakov, L. Li, *Polymers*," (in Eng) **2022**, *14*, 2117.
[8] S. Rosso, R. Meneghello, L. Biasetto, L. Grigolato, G. Concheri, G. Savio, *Addit. Manuf.* **2020**, *36*, 101713.
[9] J. Schmidt, M. A. Dechet, J. S. Gómez Bonilla, N. Hesse, A. Bück, W. Peukert, Characterization of polymer powders for selective laser sintering. Presented at the 30th Annual International Solid Freeform Fabrication Symposium Austin, Texas **2019**.
[10] I. Gibson, D. Rosen, B. Stucker, *Additive manufacturing technologies: 3D printing, rapid prototyping, and direct digital manufacturing*, Springer, New York **2014**.
[11] M. Salmi, *Materials* **2021**, *14*, 191 https://www.mdpi.com/1996-1944/14/1/191
[12] S. H. Khajavi, J. Partanen, J. Holmström, *Comput. Ind* **2014**, *65*, 50.

[13] C. Ghimouz, J. P. Kenné, L. A. Hof, *Mater. Des.* **2023**, *233*, 112224.
[14] S. C. Ligon, R. Liska, J. Stampfl, M. Gurr, R. Mülhaupt, *Chem. Rev.* **2017**, *117*, 10212.
[15] G. Wang, P. Wang, Z. Zhen, W. Zhang, J. Ji, *Mater. Des.* **2015**, *87*, 656.
[16] A. S. D. Shackleford, R. J. Williams, R. Brown, J. R. Wingham, C. Majewski, *Addit. Manuf.* **2021**, *46*, 102132.
[17] R. Seltzer, F. M. de la Escalera, J. Segurado, *Mater. Sci. Eng., A* **2011**, *528*, 6927.
[18] A. Wörz, K. Wudy, D. Drummer, A. Wegner, G. Witt, *J. Polym. Eng.* **2018**, *38*, 573.
[19] ISO 4892-3:2016 Plastics—Methods of exposure to laboratory light sources—Part 3: Fluorescent UV lamps. ISO 4892-3:2016, ISO, 2016–02 2016 https://www.iso.org/standard/67793.html
[20] T. Puttonen, M. Salmi, J. Partanen, *Polym. Test.* **2021**, *104*, 107376.
[21] Standard test method for tensile properties of plastics D638. ASTM **2014**.
[22] D. T. Pham, K. D. Dotchev, W. A. Y. Yusoff, *Proc. Inst. Mech. Eng., Part C* **2008**, *222*, 2163.
[23] EOS, Material data sheet PA 2200 Balance. Accessed from 25, May 2024. https://www.eos.info/en-us/polymer-solutions/polymer-materials/data-sheets/mds-pa-2200-balance.
[24] F. Paolucci, D. Baeten, P. C. Roozemond, B. Goderis, G. W. M. Peters, *Polymer* **2018**, *155*, 187.
[25] K. Wudy, D. Drummer, *Addit. Manuf.* **2019**, *25*, 1.
[26] B. Haworth, N. Hopkinson, D. Hitt, X. Zhong, *Rapid Prototyp. J* **2013**, *19*, 28.
[27] AMTechnologies, WHITEPAPERS & CASE STUDIES. Accessed from 15, September 2022. https://amtechnologies.com/resources/
[28] Q-LAB, Q-SUN XE-3 XENON TEST CHAMBER. Accessed from 18, October 2022. https://www.q-lab.com/en-gb/products/q-sun-xenon-arc-test-chambers/q-sun-xe-3
[29] Q-LAB, Sunlight, weathering & light Stability testing—TECHNICAL BULLETIN LU-0822. https://www.q-lab.com/documents/public/cd131122-c252-4142-86ce-5ba366a12759.pdf
[30] M. Faes, Y. Wang, P. Lava, D. Moens, Variability in the mechanical properties of laser sintered PA-12 components. Proceedings of the 26th annual international solid freeform fabrication symposium. Solid freeform fabrication symposium pp. 847–856, 2015.
[31] R. D. Goodridge, R. J. M. Hague, C. J. Tuck, *Polym. Test.* **2010**, *29*, 483.
[32] A. Pilipović, P. Ilinčić, A. Bakić, J. Kodvanj, *Polymer* **2022**, *14*, 2355 https://www.mdpi.com/2073-4360/14/12/2355
[33] H. Abdi, L. J. Williams, *Encyclopedia of Res. Des.* **2010**, *3*, 1.
[34] J. E. Cavanaugh, A. A. Neath, *Comput. Stat.* **2019**, *11*, e1460.
[35] S. Liu, A. H. Welsh, in *International encyclopedia of statistical science* (Ed: M. Lovric), Springer Berlin Heidelberg, Berlin, Heidelberg **2011**, p. 1206.
[36] R. D. Cook, in *International encyclopedia of statistical science* (Ed: M. Lovric), Springer Berlin Heidelberg, Berlin, Heidelberg **2011**, p. 301.
[37] Y. Guo, K. Jiang, D. L. Bourell, *Polym. Test.* **2015**, *42*, 175.
[38] B. Caulfield, P. E. McHugh, S. Lohfeld, *J. Mater. Process. Technol.* **2007**, *182*, 477.
[39] R. D. Goodridge, C. J. Tuck, R. J. M. Hague, *Prog. Mater. Sci.* **2012**, *57*, 229.
[40] J. Zhang, A. Adams, *Polym. Degrad. Stab.* **2016**, *134*, 169.
[41] V. Venoor, J. H. Park, D. O. Kazmer, M. J. Sobkowicz, *Polym. Rev.* **2021**, *61*, 598.
[42] B. Sanders, E. Cant, H. Amel, M. Jenkins, *Polymer* **2022**, *14*, 2682.
[43] D. Feldman, *J. Polym. Environ.* **2002**, *10*, 163.
[44] A. Touris, A. Turcios, E. Mintz, S. R. Pulugurtha, P. Thor, M. Jolly, U. Jalgaonkar, *Results Mater.* **2020**, *8*, 100149.

## SUPPORTING INFORMATION

Additional supporting information can be found online in the Supporting Information section at the end of this article.

**How to cite this article:** C. Ghimouz, J. P. Kenné, L. A. Hof, *J. Appl. Polym. Sci.* **2024**, *141*(42), e56091. https://doi.org/10.1002/app.56091